

Preliminary communication / Communication

## Originally prepared carbon-based honeycomb monoliths with potential application as VOCs adsorbents

José Manuel Gatica<sup>a</sup>, José María Rodríguez-Izquierdo<sup>a</sup>, Daniel Sánchez<sup>a</sup>,  
Tarik Chafik<sup>b</sup>, Sanae Harti<sup>b</sup>, Hicham Zaitan<sup>b</sup>, Hilario Vidal<sup>a,\*</sup>

<sup>a</sup> Departamento C.M., I.M. y Química Inorgánica, Universidad de Cádiz, Puerto Real 11510, Spain

<sup>b</sup> Laboratoire de génie chimique et valorisation des ressources,  
faculté des sciences et techniques, université Abdelmalek-Essaadi, BP 416 Tanger, Maroc

Received 29 September 2005; accepted after revision 2 February 2006

Available online 10 March 2006

### Abstract

Integral 90 wt% carbon-honeycomb lab-scale monoliths prepared from coal are characterized and applied to adsorb *o*-xylene. Textural characterization shows that the monoliths obtained after activation of the carbon exhibit appropriate porosity for their use as adsorbents. Their total capacity to retain *o*-xylene proves to be similar to that previously reported for studies under dynamic conditions on activated carbons but in the form of powder. **To cite this article:** *J.M. Gatica et al., C. R. Chimie 9 (2006)*.  
© 2006 Académie des sciences. Published by Elsevier SAS. All rights reserved.

### Résumé

Des monolithes à base de 90 % en poids de carbone en forme de nid d'abeille, préparés à l'échelle du laboratoire, ont fait l'objet d'études de caractérisation physicochimique et d'évaluation de leur capacité d'adsorption vis-à-vis de l'*o*-xylène. Les résultats de la caractérisation texturale ont montré que les monolithes obtenus après activation possèdent une porosité permettant leur utilisation comme adsorbants. Les tests d'adsorption ont montré que ces monolithes possèdent une capacité d'adsorption similaire à celle trouvée dans la littérature pour les solides sous forme de poudre à base de carbone activé étudiés en conditions dynamiques. **Pour citer cet article :** *J.M. Gatica et al., C. R. Chimie 9 (2006)*.  
© 2006 Académie des sciences. Published by Elsevier SAS. All rights reserved.

**Keywords:** Carbon monoliths; Dynamical adsorption; Breakthrough curves; FTIR analysis; *o*-Xylene

**Mots clés :** Monolithes de carbone ; Adsorption dynamique ; Courbes de percée ; Analyses IRTF ; *o*-Xylène

### 1. Introduction

Nowadays, emission to air of volatile organic compounds (VOCs), compounds with vapor pressures

greater than 133.3 Pa (1 mmHg) at room temperature, is considered one of the most concerning forms of atmospheric pollution due to their multiple harmful effects (viz. toxic character, formation of ozone) [1a]. They can be released from industrial processes using solvents, polymers and resins such as those involved in painting and coating operations. Along with catalysis, adsorption is an established abatement technology,

\* Corresponding author.

E-mail address: [hilario.vidal@uca.es](mailto:hilario.vidal@uca.es) (H. Vidal).

activated carbons being one of the best candidates for such application [2]. Usually, carbon-based adsorbents are rather employed as beds of powdered or granulated materials than in the monolithic form as the rheological properties of carbon make it a complicated material for processing through extrusion. Nonetheless, compared with the conventional packed beds, monolithic structures offer well-known advantages for processes where pressure drop has a significant economic impact. In addition, monoliths represent an easier handling design [1b].

To the best of our knowledge, the studies of honeycomb monoliths of activated carbons found in literature correspond to the use of carbon as deposited on a ceramic monolith [3,4], and thus not introduced before extrusion, or if extruded, either there is no indication of how extrudability of the carbonaceous paste is finally achieved or carbon used is not the major component or derives from a polymeric resin instead of consisting of natural coal [5–7]. Other strategy is the use of cellulose with the desired structure which is subjected to impregnation with pitch as carbon precursor [8]. There is no doubt that the topic still attracts, as new and refined methods are reported. In this regard, recently a carbon monolith (although not in the honeycomb form) was synthesized as a replica of a tailored-pore silica monolith by using a complex and time-consuming method based on templating procedure and sol-gel process [9].

In this sense, we have recently extended preparation methods based on the techniques that are usually employed with ceramic materials to carbonaceous pastes, what has allowed us to obtain, among other compositions, integral 90 wt% carbon-honeycomb lab-scale monoliths starting from coal [10]. This original experimental approach only implies, in contrast to other methods, the measurement of plastic properties just related with the humidity of the paste to be extruded [11]. The monoliths hereby obtained can be further modified by subsequent activation. Mechanical and textural properties of the resulting monoliths have been studied here, the latter being correlated with their adsorptive performance which is illustrated through an application to adsorption of a model VOC pollutant such as *o*-xylene.

## 2. Experimental

### 2.1. Materials

The honeycomb square section monoliths (with 4 cells  $\text{cm}^{-2}$ , in a  $2 \times 2$  configuration) tested in the present work were prepared from natural coal provided by

the National Institute of Carbon in Spain, whose composition was 30 wt% of volatile and less than 6 wt% of ashes, and 75 vol% of vitrinite phase concerning its maceral composition. Elemental analysis of the coal gave the following results: C (72.7 wt%), H (1.8 wt%), N (0.3 wt%) and S (0.1 wt%). As it presented initially a high average particle size (3 mm), it was crushed and sieved until its conversion into grains finer than 250  $\mu\text{m}$ .

### 2.2. Carbon-based monoliths preparation

The honeycomb monoliths here prepared were obtained by means of extrusion of a carbon-based material. To obtain a dough with adequate rheological properties for the extrusion, some additives were used besides water: 9.5% silicate clay (ARGI-2000 from VICAR, S. A.), 2.5% glycerine, 1.9% methylcellulose and 0.3% aluminum phosphate dissolved in *o*-phosphoric acid (weight percentages referred to the extrudable paste excluding water). Measurement of the liquid limit (LL) and plasticity index (PI) of different samples allowed, in a previous stage, to optimize the composition of the paste until it fulfilled simultaneously the extrudability prerequisites,  $40\% < \text{LL} < 60\%$  and  $10\% < \text{PI} < 30\%$ . Thus,  $\text{LL} = 47\%$  and  $\text{PI} = 24\%$  were obtained for the above described paste. After its final extrusion, the green monoliths were dried in an oven at 80 °C overnight, and then underwent a thermal treatment consisting, first, of a preoxidation (air, 250 °C, 24 h) in order to prevent a pseudoplastic state by oxygenated cross-links, which allows further activation and pore development [12]. Subsequently, carbonization (Ar, 840 °C, 1 h) and activation ( $\text{H}_2\text{O}$ , 250 Torr/Ar, 860 °C, up to a burn-off degree of 15 wt%) treatments were carried out to eliminate the additives and to develop the porous structure required for application of the monoliths as adsorbents. Further details of the experimental methodology to obtain coal-based honeycomb monoliths have been previously reported [10]. Fig. 1 shows an image of a typical monolith obtained by the above described procedure.

### 2.3. Characterization techniques

Textural characterization of both the starting material and the final activated monoliths has been carried out by measuring true and apparent densities (mercury at 0.1 MPa), mercury porosimetry and physical adsorption of  $\text{N}_2$  at  $-196$  °C (Table 1). For this study, a Micromeritics 1320 Autopycnometer, a Macropores Unit 120

Table 1  
Textural properties of the samples

Sample	$S_{\text{BET}}$ (m <sup>2</sup> /g)	$\rho_{\text{He}}$ (g/cm <sup>3</sup> )	$\rho_{\text{Hg}}$ (g/cm <sup>3</sup> )	$\varepsilon^*$ (%)	Pore volume (cm <sup>3</sup> g <sup>-1</sup> )		
					Micro <sup>a</sup>	Meso <sup>b</sup>	Macro <sup>c</sup>
Natural coal	3	1.440	0.857	40.5	0.000	0.000	0.122
Activated coal-based monolith	487	2.040	0.836	59.0	0.154	0.008	0.161

\* $\varepsilon$  represents the open porosity and has been calculated as:  $\varepsilon = (1 - \rho_{\text{Hg}}/\rho_{\text{He}}) \times 100$ .

<sup>a</sup> Total micropores (pore diameter,  $w < 2$  nm) evaluated from DFT applied to N<sub>2</sub> adsorption isotherms at -196 °C;

<sup>b</sup> Mesopores ( $2 < w < 50$  nm) from DFT applied to N<sub>2</sub> adsorption isotherms at -196 °C;

<sup>c</sup> Macropores ( $w > 50$  nm) evaluated from mercury porosimetry.

from Carlo Erba, and a Micromeritics ASAP 2010, have been used, applying the methods and experimental protocols reported elsewhere [13]. The isotherms were used to calculate the specific surface area,  $S_{\text{BET}}$ , and pore size distributions. SEM micrographs have been obtained using a SIRION-FEG Scanning Electron Microscope (Philips) with a nominal resolution of 1.5 nm. Mechanical resistance of the monoliths has been also measured employing a NESTOR Universal Machine for Mechanical Assays capable of working at a maximum pressure of 100 kN.

*o*-Xylene adsorption/desorption experiments were performed under dynamic conditions at atmospheric pressure with a homemade device as reported in [14]. Nitrogen was used as gas carrier for *o*-xylene with a gas mixture flow rate of 100 cm<sup>3</sup> min<sup>-1</sup> and a pollutant concentration of 0.36%. The adsorption tests were carried out at 27 °C over around 1 g of monolith sample previously subjected to an in situ treatment in N<sub>2</sub> flow (100 cm<sup>3</sup> min<sup>-1</sup>) at 210 °C. After sample saturation, the gas mixture was switched to a 100 cm<sup>3</sup> min<sup>-1</sup> of N<sub>2</sub> flow in order to proceed with isothermal desorption at 27 °C until the *o*-xylene concentration in the gas phase reached zero, followed by a temperature programmed desorption (TPD) experiment using a heating rate of 5 °C min<sup>-1</sup>. Composition of the gas mixture at the out-

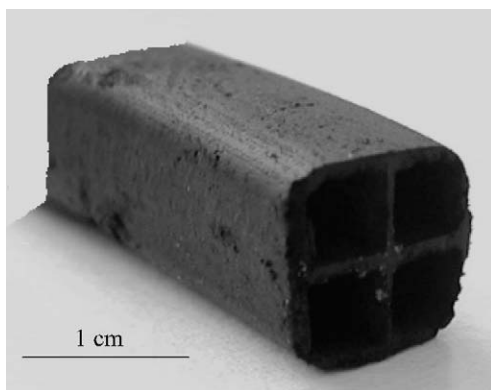


Fig. 1. Image of a typical carbon-based monolith obtained in this work.

let of the stainless steel tube that contained the sample was continuously monitored by FTIR spectrometry (Jasco 410, resolution 4 cm<sup>-1</sup>). Further details of this methodology are described in [14].

### 3. Results and discussion

#### 3.1. Textural and mechanical properties

As Fig. 2 shows the N<sub>2</sub> adsorption/desorption process on the final activated monoliths is described by a type I isotherm in good agreement with previous references for carbon honeycombs obtained by means of other procedures different from ours, briefly summarized in the introduction [4,7,8].

A general overview of the textural properties including data obtained with other characterization techniques not only for the final monoliths but also for the starting natural coal is offered in Table 1. As expected, activa-

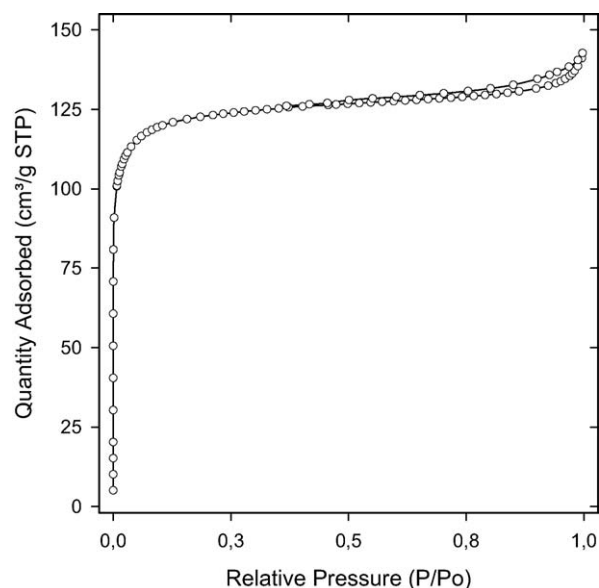


Fig. 2. Nitrogen adsorption/desorption isotherm of the activated-carbon-based monoliths.

tion of the green monoliths gives rise to a development of the porous network, with a remarkable increase in the open porosity. In fact, this result confirms that the preoxidation treatment, previously tested on powdered samples [12], is also suitable for monoliths. In the same way, a huge increase in the BET surface area is observed with regard to the starting carbon material. This is undoubtedly of great interest and innovative, since it points out that samples containing carbon as the major component but in a monolithic design and presenting attractive textural properties have been accomplished. Concerning the pore volume distribution, the microporosity—initially negligible in the coal carbon—clearly increases due to the activation step, accounting for up to 47% of the total porosity in the activated monoliths. Also remarkable, the monoliths prepared seem to exhibit a bimodal distribution of the pores in the sense that they also present a high content of macropores, typical of extrudates as a consequence of the removal of the binders during carbonization and activation; mesopores are practically absent.

Fig. 3 shows a SEM image corresponding to the monolith wall allowing the textural characterization at micron-sized scale of the material. It can be observed that the carbon-based samples after being extruded and activated display a conglomerate of particles heterogeneous in size. The SEM data also show evidences of macroporosity in agreement with the textural results.

According to the mechanical assays, the monoliths present a resistance to breaking under pressure along the channels direction of 1.37 MPa. This value, although considerably lower than those reported for carbon-coated cordierite [3] or carbon-ceramic composites [5] can be considered acceptable for their application as adsorbents considering that in our case the carbon constitutes the matrix of the monolith. According

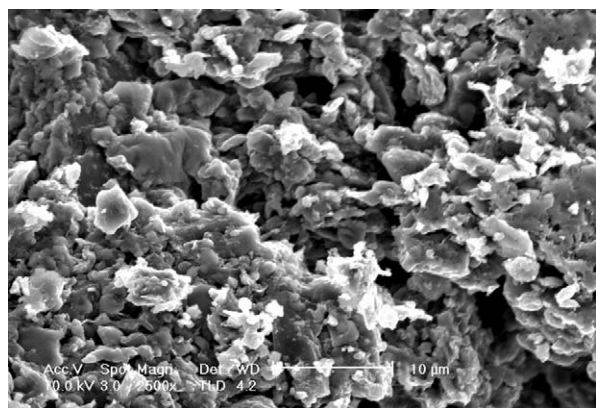


Fig. 3. Scanning electron micrograph obtained for the carbon-based monoliths after activation.

to our results, the mechanical strength of the samples prepared differs in relation to the experimental conditions employed in the activation of the monoliths, so an optimization of this property can be performed in balance with the target porosity during the scaling to bench conditions of the lab samples.

### 3.2. Adsorptive behavior

Fig. 4 represents the evolution of the *o*-xylene IR bands during the adsorption experiment on the activated monoliths. Similar spectra were recorded for the isothermal desorption and TPD (results not shown). No other IR bands than those attributable to *o*-xylene were detected, thus indicating there is no transformation of the adsorbed phase. This information derived from the use of FTIR as analysis technique can be considered an additional benefit of our experimental approach to this kind of adsorption studies. A numerical treatment of the integrated absorbance data from *o*-xylene IR bands, according to the procedure described below, leads to the breakthrough, isothermal desorption and TPD curves shown in Fig. 5. These curves allowed us to obtain the total *o*-xylene uptake as well as the amount reversibly and irreversibly adsorbed by the sample. Total uptake was calculated from the area between curves corresponding to adsorption experiments without and with monolith, respectively (Fig. 5(1)). Reversible adsorption was estimated from blank desorption experi-

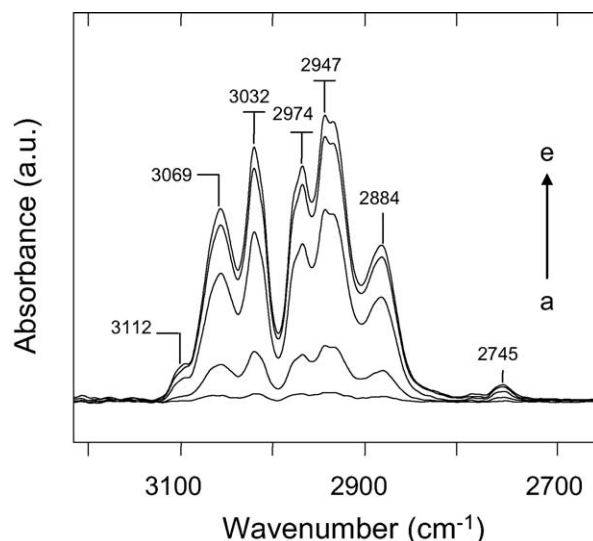


Fig. 4. Evolution of the *o*-xylene IR bands during the adsorption experiment on the carbon-based monoliths, performed at 27 °C using an *o*-xylene (3600 ppm)/N<sub>2</sub> mixture, after (a–e): 3.5, 27, 58, 80 and 95 min. For the sake of clarity, only some of the IR spectra registered during the tests are shown.

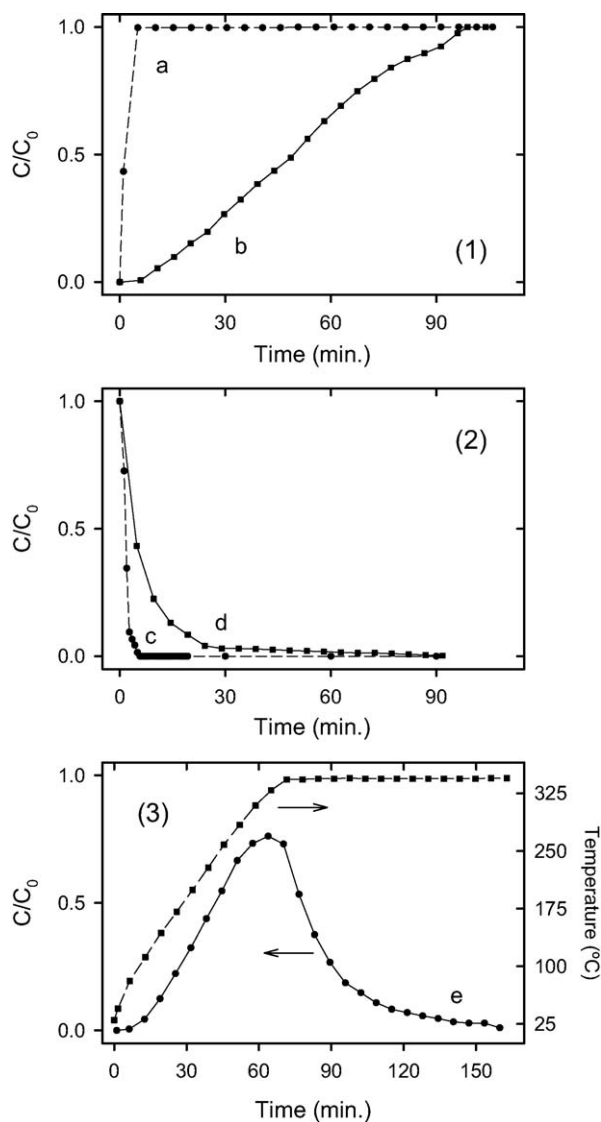


Fig. 5. 1) Adsorption of *o*-xylene (3600 ppm)/N<sub>2</sub> at 27 °C on the carbon-based monolith: blank response (a) and breakthrough (b) curves; 2) *o*-Xylene isothermal desorption at 27 °C under N<sub>2</sub> flow after the adsorption step: Blank response (c) and curve obtained from the monolith (d); and 3) TPD after the isothermal step desorption (e). Integrated absorbance of the *o*-xylene IR bands normalized data are shown.

ments, and *o*-xylene desorption from the monolith at 27 °C (Fig. 5(2)). Irreversible adsorption was determined from TPD experiments heating the monolith up to 350 °C and maintaining this temperature until total desorption of the *o*-xylene (Fig. 5(3)).

Table 2 summarizes the quantitative results obtained in the above mentioned study. As we can see, the tested monoliths exhibit a total capacity to adsorb *o*-xylene around 550 μmol g<sup>-1</sup>, a value in the range of those

Table 2

Study of the *o*-xylene adsorption capacity at 27 °C of the carbon-based monoliths

Cycle	Total adsorption (μmol g <sup>-1</sup> )	Reversible adsorption (μmol g <sup>-1</sup> ) <sup>a</sup>	T <sub>m</sub> (°C) <sup>b</sup>	E <sub>d</sub> (kJ mol <sup>-1</sup> ) <sup>c</sup>
1	580	61	335	157
2	561	62	340	159
3	546	68	335	158

<sup>a</sup> As determined by means of isothermal desorption at 27 °C;

<sup>b</sup> Temperature of the peak maximum in the TPD experiments;

<sup>c</sup> Activation energy of the desorption process.

previously reported for powdered activated carbons studied under similar experimental conditions [15]. It is also remarkable that this value, when converted into cm<sup>3</sup> g<sup>-1</sup>, represents about 43% of the total micropore volume shown in Table 1. This would mean that an important fraction of the monolith micropores remain empty and might therefore constitute a potential storage place for other pollutants or even more *o*-xylene molecules under different experimental conditions. In addition, it is to be noted that, according to Fig. 5, total regeneration of the material would require its heating at 350 °C. The same set of adsorption/desorption experiments was carried out three times in total, proving the stability of the monoliths. The TPD curve also allows to calculate the activation energy of the desorption process according to

$$E_d = RT_m \left[ \ln \left( \frac{v}{\beta} \right) - \ln \left( \frac{\ln v / \beta}{T_m} \right) \right]$$

considering a pre-exponential factor of  $v = 10^{13} \text{ s}^{-1}$  and the absence of readsorption, and where  $R$  is the ideal gas constant,  $\beta$  is the heating rate and  $T_m$  is the temperature of the peak maximum. The relatively high value of the activation energy shown in Table 2 is in good agreement with the aforementioned result and remains approximately the same for the different cycles suggesting the stability of the material concerning its adsorption properties and the efficiency of the regenerating treatment referred to above.

A final interesting observation derives from the analysis of the breakthrough curve in Fig. 5(1). If we compare the profile of this curve with those obtained by Gadkaree for adsorption of other volatile organic compounds such as butane or toluene on carbon honeycomb structures [4], we find a clear similarity. Nevertheless, it is convenient to remind that the kinetics of the adsorption process on monolithic samples is controlled by the space velocity which affects the slope of the curve. In spite of this, we can also say that the curve of our monoliths is similar to those obtained from packed beds



and so there does not seem to be a heavy penalty associated with using an open honeycomb structure with straight flow channels and low pressure drop in terms of adsorption behavior.

#### 4. Conclusions

In the present work, carbon-based lab-scale honeycomb monoliths have been prepared following a new methodology based in an original development for ceramics.

Both textural characterization and analysis by SEM show that the monoliths obtained after activation of the carbon exhibit high porosity. Measurement of the mechanical resistance gives values that appear acceptable for the scaling to bench conditions.

Tests of adsorption of *o*-xylene indicate that the monoliths prepared here have good possibilities to be used as filters of VOCs, having a total capacity to adsorb the pollutant around  $550 \mu\text{mol g}^{-1}$  which is similar to that previously reported for other active carbons but in the form of powdered designs. In addition, the adsorption capacity remains constant along several cycles of adsorption/regeneration and seems to be kinetically efficient according to the breakthrough curves.

Finally, we have demonstrated that the methodology based on FTIR analysis which we have developed to estimate the adsorption capacity of powdered samples in a previous work [14], is also valid for monolithic adsorbents. In that case, diatomite mineral was proved to exhibit interesting efficiency for volatile organic compounds removal. In the light of such result and those obtained here, we are planning to apply this original method for adsorption characteristics investigations to other natural clays-based monoliths.

#### Acknowledgements

This work has been funded by the 1FD97-1085-CO2-O2 CICYT Project of the Science and Technology Ministry of Spain and the A46/02 Project of the Junta de Andalucía (Spain). The authors acknowledge the Central Service of Science and Technology of the University of Cadiz for the use of its SEM facilities, and also gratefully recognize the valuable help provided by Dr. José Bernardo Parra and Concepción Ania from the Instituto Nacional del Carbon (CSIC) in Spain.

#### References

- [1] R.M. Heck, R.J. Farrauto, S.T. Gulati, Catalytic air pollution control, Commercial technology, Wiley, New York, 2002 [(a) pp. 281–305; (b) pp. 11–24].
- [2] W.H. Lee, P.J. Reucroft, Carbon 37 (1) (1999) 7.
- [3] T. Valdés-Solís, G. Marbán, A.B. Fuertes, Micropor. Mesopor. Mater. 43 (2001) 113.
- [4] K.P. Gadkaree, Carbon 36 (7–8) (1998) 981.
- [5] M. Yates, J. Blanco, P. Avila, M.P. Martín, Micropor. Mesopor. Mater. 37 (2000) 201.
- [6] F.D. Yu, L.A. Luo, G. Grevillot, J. Chem. Eng. Data 47 (2002) 467.
- [7] S.R. Tennison, Appl. Catal. A: General 173 (2) (1998) 289.
- [8] J. Alcañiz-Monge, C. Blanco, A. Linares-Solano, R. Brydson, B. Rand, Carbon 40 (4) (2002) 541.
- [9] Z. Shi, Y. Feng, L. Xu, S. Da, M. Zhang, Carbon 41 (13) (2003) 2677.
- [10] J.M. Gatica, J.M. Rodríguez-Izquierdo, D. Sánchez, C.O. Ania, J.B. Parra, H. Vidal, Carbon 42 (2004) 3251.
- [11] J.M. Rodríguez-Izquierdo, H. Vidal, J.M. Gatica, D. Sánchez, A.A. Córdón, Inventors, University of Cádiz, Spain. ES Patent 2221782 B1, issued 16 December 2005.
- [12] J.B. Parra, J.J. Pis, J.C. de Sousa, J.A. Pajares, R.C. Bansal, Carbon 34 (6) (1996) 783.
- [13] J.J. Pis, J.B. Parra, G. de la Puente, F. Rubiera, J.A. Pajares, Fuel 77 (6) (1998) 625.
- [14] H. Zaitan, T. Chafik, C. R. Chimie 8 (2005) 1701.
- [15] C.M. Wang, K.S. Chang, T.W. Chung, H. Hu, J. Chem. Eng. Data 49 (2004) 527.